Viriditoxin regulates apoptosis and autophagy via mitotic catastrophe and microtubule formation in human prostate cancer cells

SOMA KUNDU[1], TAE HYUNG KIM[2], JUNG HYUN YOON[1], HAN-SEUNG SHIN[3], JAEWON LEE[1], JEE H. JUNG[1] and HYUNG SIK KIM[2]

[1]Laboratory of Marine Natural Product, College of Pharmacy, Pusan National University, Busan 609-735; [2]Laboratory of Molecular Toxicology, School of Pharmacy, Sungkyunkwan University, Suwon 440-746; [3]Department of Food Science and Biotechnology, Dongguk University-Seoul, Seoul 100-715, Republic of Korea

Received June 26, 2014; Accepted August 4, 2014

DOI: 10.3892/ijo.2014.2659

Abstract. Microtubule targeting chemicals are considered excellent antitumor drugs through their binding to tubulin, which affects the instability of microtubules resulting in arrest of cancer cells. The present study was designed to investigate the antitumor effects of viriditoxin (VDT) against human prostate cancer cells. VDT, isolated from *Paecilomyces variotii* fungus, which was derived from the jellyfish *Nemopilema nomurai*, offers a new approach for controlling resistant bacterial infections by blocking bacterial cell division proteins. VDT produced dose-dependent cytotoxicity against human prostate cancer cells. Treatment with VDT promoted both apoptosis and autophagy in LNCaP cells. Annexin V/FITC staining indicated that apoptosis occurred in VDT-treated LNCaP cells. DAPI staining revealed morphological changes in the cell nuclei indicative of mitotic catastrophe in LNCaP cells. VDT caused cell growth inhibition via G2/M phase arrest. Moreover, VDT also increased autophagic cell death in LNCaP cells by induction of several autophagy-related proteins such as LC3 II, Atg5, Atg7 and beclin-1 protein, which are essential for autophagy induction. These results were also confirmed by acridine orange staining. This study indicates that VDT could potentially be effective against prostate cancer by promoting multiple modes of growth arrest and cell death coupled with apoptosis and autophagy.

Correspondence to: Professor Jee H. Jung, Laboratory of Marine Natural Product, College of Pharmacy, Pusan National University, Busan 609-735, Republic of Korea
E-mail: jhjung@pusan.ac.kr

Professor Hyung Sik Kim, Laboratory of Molecular Toxicology, School of Pharmacy, Sungkyunkwan University, 2066, Seobu-ro, Jangan-gu, Suwon, Gyeonggi-do, 440-746, Republic of Korea
E-mail: hkims@skku.edu

Key words: viriditoxin, tubulin, microtubule, docetaxel, apoptosis, autophagy

Introduction

Prostate cancer is currently the most common and frequently occurring malignant disease throughout the world. It is estimated that prostate cancer is the second leading cause of death among men in the USA (1,2). A recent study reported that prostate cancer patients have a higher risk of death due to causes other than prostate cancer itself (3). Despite the serious implications of prostate cancer, little is known about the molecular mechanism underlying this disease. To date, only a few risk factors have been clearly established for prostate cancer including age, a genetic history, and a complex interplay between environmental factors such as lifestyle and diet (4,5). Chemotherapy remains one of the major options for effective treatment of hormone refractory prostate cancer (HRPC). The ultimate goal of successful chemotherapy is simultaneous suppression of survival signaling circuits of cancer cells with minimal toxicity to normal cells.

Viriditoxin (VDT) has been isolated from *Paecilomyces variotii* fungus (derived from the jellyfish *Nemopilema nomurai*) and offers a new approach for controlling antibiotic-resistant bacterial infection (6-8). Bacterial cell division is modulated by a group of proteins called divisomes. The filamenting temperature-sensitive mutant Z (FtsZ) is one of these proteins and plays a key role in its own cell division. VDT inhibits FtsZ by affecting cell morphology, macromolecular synthesis and DNA damage responses; thus, more recently, FtsZ has been considered as a novel therapeutic target of antibiotics (8). FtsZ is also a close structural homologue of eukaryotic tubulin, which forms microtubules during cell division and plays a critical role in the cytokinesis of cells (9). Therefore, we hypothesized that VDT may also inhibit eukaryotic cell division by blocking tubulin. Evidence shows that, after testing several compounds using SRB assays, the NSC159628 (VDT) compound causes cell cycle arrest at the G2/M phase after 12 h of treatment. In addition, when cells are further treated for more than 24 h, NSC159628 induces apoptosis in HeLa cells (10).

Microtubules are major dynamic structural components of cytoskeleton formation during cell development, mainte-

nance of cell shape, cell division, intracellular transport and cell movement (11). Microtubule binding drugs are used as anticancer agents for the treatment of a variety of cancers. Different types of microtubule stabilizing agents including taxol, docetaxel and paclitaxel have been shown to have potent anticancer activity against various types of human cancers (12,13). Now, it is widely believed that, like taxol, docetaxel binds to β-tubulin, stabilizes spindle microtubules, and impairs mitosis by retarding cell cycle progression in the G2/M phase (14). Moreover, evidence has revealed that p53, a tumor suppressor gene, plays an important role in apoptosis in prostate and colorectal cancer cells after treatment with microtubule-targeting agents (15). In spite of the clear relationship between mitotic mechanisms and apoptosis, tumor suppression by p53 has been generally accepted as a predominant mechanism of cell death in response to chemotherapy drugs targeting microtubules (16-18). Mitotic catastrophe can also be triggered by microtubule instability leading to an abnormal mitotic checkpoint (19). Mitotic catastrophe is a mechanism of cell death characterized by the occurrence of aberrant mitosis and is induced by improper chromosomal segregation and cell division with characteristic features of polynucleated cells (20). It results from premature or inadequate entry of cells into mitosis and represents an intermediate stage between prolonged mitotic arrest and the induction of cell death (19). Stilbene 5c, a stilbene derivative, is a potentially potent antitumor agent that acts by binding to tubulin. Stilbene 5c was shown to simultaneously trigger multiple mechanistic pathways leading to cell death including the promotion of apoptosis, autophagic cell death and mitotic catastrophe (21). Microtubules play an important role in autophagy through their association with autophagosomes. A previous study showed that microtubule disruption induced by nocodazole or vinblastine dramatically inhibits autophagy-mediated protein degradation (22) or delays the transport of proteolytic enzymes to the lysosome (23). In contrast, microtubules facilitate autophagosome formation (24) and microtubule depolymerizing agents, such as naphthazarin, induce autophagy in A549 lung cancer cells (25). Also, evidence has shown that different microtubular interfering agents enhance the fusion of autophagosomes by acetylation of microtubules (26). However, the exact role of microtubules in autophagic cell death is still unclear. Thus, we investigated the antitumor effect of VDT against prostate cancer cells. According to our data, VDT effectively inhibited proliferation of prostate cancer cells through the induction of cell cycle arrest at the G2/M phase and autophagic cell death.

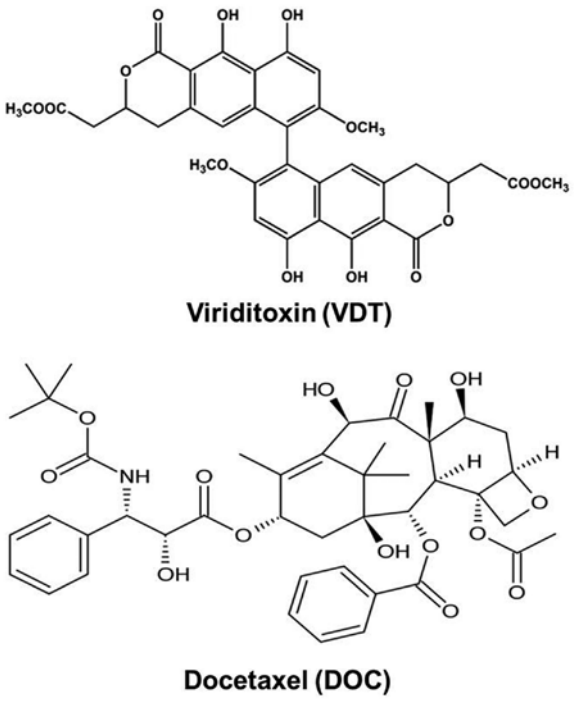

Figure 1. Chemical structure of viriditoxin (VDT) and docetaxel (DOC).

Materials and methods

Chemicals and reagents. The novel compound VDT was kindly provided by Professor Jee H. Jung, Laboratory of Marine Natural Products, College of Pharmacy, Pusan National University, South Korea (Fig. 1). Reference compound docetaxel (DOC, cat. no. 01885) was purchased from Sigma-Aldrich (St. Louis, MO, USA). Medium (RPMI-1640, cat. no. 11875), antibiotics (Antibiotic-Antimycotic, cat. no. 15240), HEPES (cat. no. 15630-080), Dulbecco's phosphate-buffered saline (DPBS, cat. no. 21600-010), trypsin-EDTA (cat. no. 15400) and fetal bovine serum (FBS, cat. no. 16000) were purchased from Gibco Invitrogen Corporation (Carlsbad, CA, USA). Primary antibodies against cyclin A (sc-751), cyclin B1 (sc-245), cyclin E (sc-481), cyclin-dependent kinases 2 (Cdk2, sc-6248), Cdk4 (sc-260), Cdc2 (sc-954), poly-ADP-ribose polymerase (PARP, sc-7150), Bax (sc-7480), Bcl-2 (sc-7382), cytochrome *c* (sc-7159), p53(sc-126) and p21 (sc-6246) as well as horseradish peroxidase-conjugated secondary antibodies (sc-2004, sc-2005) were from Santa Cruz Biotechnology (Santa Cruz, CA, USA). Primary antibodies against LC3 (#3868), Atg5 (#8540), Atg7 (#2631), Beclin 1 (#3495), cleaved caspase-3 (#9664), cleaved caspase-7 (#8438) and cleaved caspase-9 (#7237) were from Cell Signaling Technology (Danvers, MA, USA). The Annexin V-FITC apoptosis detection kit I (cat. no. 556547) was purchased from BD Biosciences (San Diego, CA, USA). All other chemicals were purchased from Sigma-Aldrich. VDT and DOC were dissolved in dimethyl sulfoxide (DMSO, D2650, Sigma-Aldrich) and stored at -20˚C until use. These agents were diluted to appropriate concentrations with culture medium containing 1% FBS for all experiments. The final concentration of DMSO was less than 0.1% (vol/vol).

Cell lines and culture media. Human prostate cancer cell lines LNCaP (ATCC CRL-1740), PC3 (ATCC CRL-1435), and DU145 (ATCC HTB81) were obtained from the American Type Culture Collection (Manassas, VA, USA). The cells were grown in RPMI-1640 containing 10% heat-inactivated FBS, 1.25 mM HEPES and 100 U/ml penicillin/streptomycin. Cells were maintained as a monolayer at 37˚C in a humidified atmosphere containing 5% CO_2, and culture medium was replaced every 2 days. After 48 h of incubation, culture medium was replaced with treatment medium containing the desired concentration of drug.

Cell viability assay. Cell viability was determined using 3-(4,5-dimethylthiazol-2-yl)-2,5-diphenyl-tetrazolium bromide (MTT, M5655, Sigma-Aldrich). The cultures were seeded in 96-well plates at a density of $2x10^3$ cells per well. After 48 h of incubation, cells were treated with various concentrations of VDT or DOC and incubated for 24 and 48 h. After treatment, 15 μl of MTT reagent (5 mg/ml) was added and the cells were incubated in the dark for 4 h at 37˚C. Then, the supernatant was aspirated and formazan crystals were dissolved in 100 μl of DMSO at 37˚C for 15 min with gentle agitation. The absorbance was measured at 540 nm using the VERSA Max Microplate Reader (Molecular Devices Corp., Sunnyvale, CA, USA). Data were analyzed from three independent experiments and normalized to the absorbance of wells containing media only (0%) or untreated cells (100%). IC_{50} values were calculated from sigmoidal dose response curves using SigmaPlot 10.0 software (Systat Software, Inc., Point Richmond, CA, USA).

Western blot analysis. Cells were treated with VDT (0.1, 0.5 and 1 μM) or DOC (0.5 μM) for 48 h and then harvested by trypsinization and washed twice with cold PBS. For protein isolation, cells were suspended in PRO-PREP™ solution (cat. no. 17081, Intron, Seongnam, Korea) and placed on ice for 30 min. The suspension was collected after centrifugation at 12,000 x g for 15 min at 4˚C. To isolate cytosolic and nuclear proteins, cells were suspended in 50 μl of lysis buffer I containing 10 mM HEPES, pH 7.9, 1.5 mM $MgCl_2$ (cat. no. M8266, Sigma-Aldrich), 10 mM KCl (cat. no. P9333, Sigma-Aldrich), 0.5 mM DTT (cat. no. 43815, Sigma-Aldrich), and 0.5 mM PMSF (cat. no. 93482, Sigma-Aldrich), and placed on ice for 20 min. Supernatant was removed after centrifugation at 12,000 x g for 10 min, and the pellet was resuspended in 30 μl of lysis buffer II containing 10 mM HEPES, pH 7.9, 1.5 mM $MgCl_2$, 10 mM KCl, 0.5 mM DTT, 0.5 mM PMSF, and 0.5% NP-40 (cat. no. 74385, Sigma-Aldrich), and placed on ice for 20 min. Cells were lysed by gently vortexing, and nuclei were separated from the cytosol by centrifugation at 12,000 x g for 10 min. Nuclei were resuspended in 40 μl of buffer III containing 5 mM HEPES, pH 7.9, 300 mM NaCl (cat. no. S3014, Sigma-Aldrich), 1.5 mM $MgCl_2$, 0.2 mM EDTA (cat. no. E9884), 0.5 mM DTT, 0.5 mM PMSF, and 26% glycerol (cat. no. G2025, Sigma-Aldrich) and placed on ice with shaking for 30 min. Nuclear extracts were obtained by centrifugation at 12,000 x g for 30 min and stored at -70˚C. Protein concentration was measured with protein assay reagents (cat. no. 500-0002, Bio-Rad, Hercules, CA, USA) according to the manufacturer's instructions. Equivalent amounts of proteins were resolved on a 6-15% SDS-PAGE gradient, transferred to polyvinylidene difluoride membrane (PVDF, cat. no. IPVH00010, Millipore, Billerica, MA, USA), and probed sequentially with the primary antibodies. Proteins were visualized with horseradish peroxidase (HRP)-conjugated secondary antibodies (Santa Cruz Biotechnology) using the ECL-plus kit (cat. no. RPN2132, GE Healthcare, Pittsburgh, PA, USA) for detection.

Cell cycle analysis. Cells were treated with VDT (0.1, 0.5 and 1 μM) or DOC (0.5 μM) for 48 h. The total sample of cells, both in suspension and adhered, was harvested and washed with PBS containing 1% bovine serum albumin (BSA, cat. no. A4503, Sigma-Aldrich) before fixing in 95% ice-cold ethanol containing 0.5% Tween-20 (cat. no. P9416, Sigma-Aldrich) for at least 1 h at -20˚C. The cells ($1x10^6$) were washed in 1% BSA, stained with cold propidium iodide (PI, cat. no. P4864, Sigma-Aldrich) staining solution including 100 μg/ml ribonuclease A (RNase, cat. no. R6513, Sigma-Aldrich), and incubated in the dark for 30 min at room temperature. DNA content was analyzed by flow cytometry (BD Accuri™ C6, Becton-Dickinson, San Jose, CA, USA).

DAPI staining. Morphological changes of the nuclear chromatin of apoptotic cells were identified by staining with the DNA binding dye 4',6-diamidino-2-phenylindole (DAPI, cat. no. D8417, Sigma-Aldrich). Cells were grown in 6-well plates at a density of $1x10^5$ cells per well followed by the desired treatment. After 48 h of incubation, the cells were washed with cold PBS, fixed with methanol for 30 min, rewashed and then stained with 200 μl of DAPI solution (1 μg/ml) at 37˚C for 30 min. After removing the staining solution, apoptotic cells were visualized using a fluorescence microscope (Carl Zeiss Axiovert 200, Oberkochen, Germany).

Annexin V-FITC binding assay. An Annexin V-FITC binding assay was performed according to the manufacturer's instruction using the Annexin V-FITC apoptosis detection kit I (BD Biosciences, San Diego, CA, USA). The cells were treated with VDT or DOC for 48 h. The total number of cells was collected by trypsinization and washed twice with cold PBS. The pellet was resuspended in 100 μl of 1X binding buffer at a density of $1x10^5$ cells per ml and incubated with 5 μl of FITC-conjugated Annexin V and 5 μl of PI for 15 min at room temperature in the dark. Binding buffer (1X, 400 μl) was added to each sample tube, and immediately the samples were analyzed by FACS (Becton-Dickinson) and quantified using Cell Quest software.

Acridine orange staining. Cells were grown in cover glass bottom dishes at a density of $1x10^5$ cells per dish, cultured for 24 h, and then incubated with the indicated drug in RPMI containing 1% FBS for 48 h. Following incubation, the media was removed and the cells were stained with 1 μg/ml of acridine orange (cat. no. A8097, Sigma-Aldrich) at 37˚C for 15 min. After removing the staining solution, PBS was added to the dish and the cells were examined using a fluorescence microscope at x600 magnification (Olympus FV10i, Tokyo, Japan).

Mitotic catastrophe assay. Cells were grown in cover glass bottom dishes at a density of $1x10^5$ followed by treatment with VDT or DOC at the desired concentration. After 48 h of incubation, the cells were washed with cold PBS, fixed with 4% paraformaldehyde (cat. no. 158127, Sigma-Aldrich) and isopropanol (cat. no. I9516, Sigma-Aldrich) for 15 min, rewashed, and then stained with DAPI solution (1 μg/ml) at 37˚C for 15 min. After removing the staining solution, the cells were visualized and images were taken using a fluorescence microscope at x400 magnification (Olympus FV10i). Five separate experiments were visualized and evaluated. Cells were assigned to three groups as follows: normal nuclei; abnormal multinucleated (MN) cells characteristic of mitotic catastrophe; and apoptotic nuclei. Small round evenly stained nuclei were considered as normal nuclei and apoptotic was

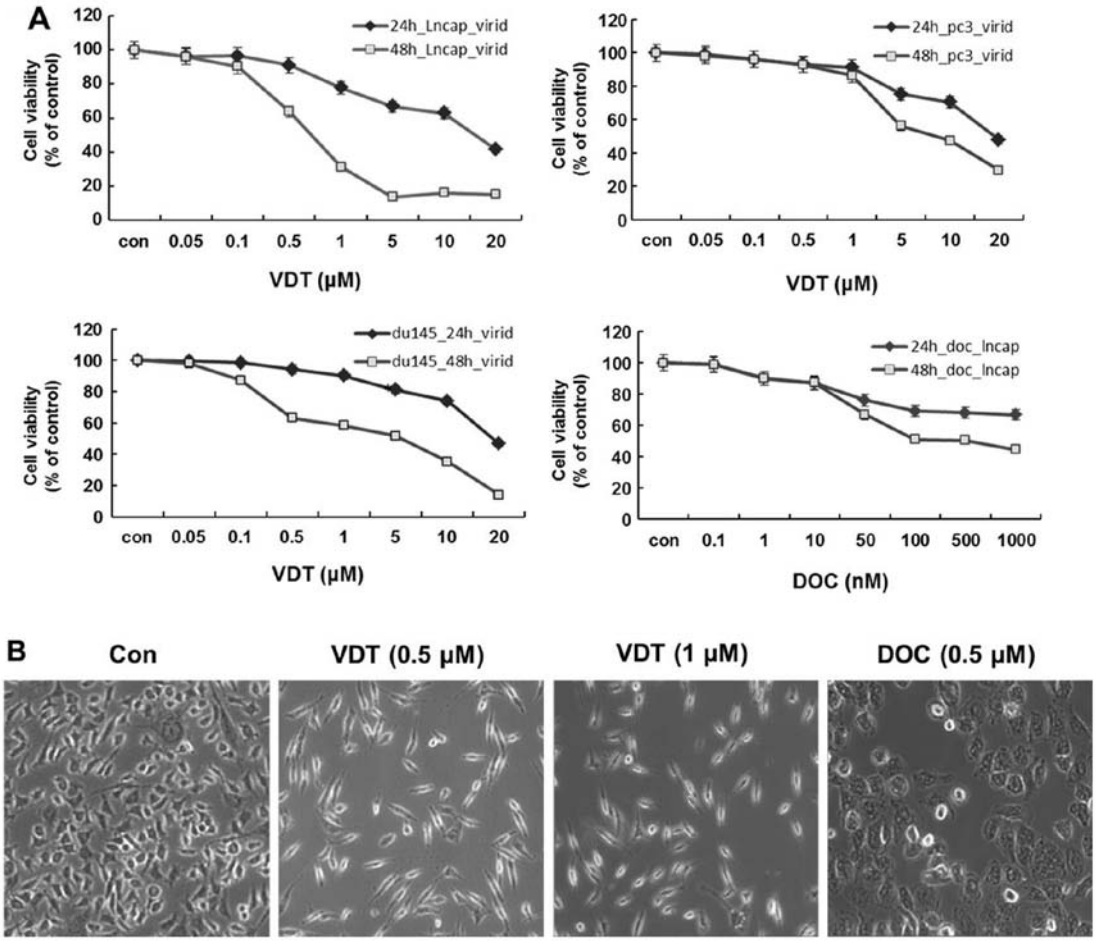

Figure 2. Cytotoxic effect of viriditoxin on three prostate cancer cell lines measured by the MTT assay. (A) LNCaP, DU145 and PC3 cells were treated with viriditoxin (VDT) at various concentrations (0.05-20 μM) for 24 and 48 h. LNCaP cells were also treated with the positive control docetaxel (DOC) for 24 and 48 h. The percentage of viable cells was determined as the ratio between treated cells and untreated controls. Results were expressed as mean ± SEM, n=3. (B) Morphological changes in LNCaP cells after treatment with VDT or DOC. Cells were treated for 48 h with the indicated concentrations of VDT or DOC. Morphological changes were observed using x100 magnification.

defined as the presence of condensed fragmented chromatin. Multinucleated enlarged nuclei, complete aberrant nuclei, catastrophic clusters and nuclei undergoing multinucleation were considered as multinucleated mitotic catastrophe nuclei (27).

Statistical analysis. All the data shown represent the mean ± SEM of triplicate experiments performed in a parallel manner unless otherwise indicated. Statistical significance was determined using the paired Student's t-test. A $p<0.05$ or $p<0.01$ was considered statistically significant.

Results

Viriditoxin inhibits the proliferation of prostate cancer cells. To determine the cytotoxicity of VDT on human prostate cancer cells, LNCaP, DU145 and PC3 cells were treated with various concentrations of VDT for 24 and 48 h. As shown in Fig. 2A, VDT significantly inhibited the growth of the three human prostate cancer cell lines in a concentration- and time-dependent manner. After 48 h of treatment, the IC_{50} values of VDT against LNCaP, DU145 and PC3 cells were 0.63, 5.36 and 7.6 μM, respectively (Table I). VDT appeared to be more potent in LNCaP cells compared to DU145 and PC3 cells. VDT treatment also induced marked morphological changes, including cytoplasmic shrinkage and cellular flattening following 48 h of treatment (Fig. 2B).

Table I. The IC_{50} values of viriditoxin on prostate cancer cell lines.

	IC_{50} values (μM)		
Time	LNCaP	DU145	PC3
24 h	14.84	18.47	18.72
48 h	0.63	5.36	7.60

LNCaP, DU145 and PC3 cells were treated with VDT at various concentrations (0.05-20 μM) for 24 and 48 h. The percentage of viable cells was determined as the ratio between treated cells and untreated controls.

VDT induces G2/M phase arrest and affects cell cycle regulatory proteins. To examine the effect of VDT on cell cycle progres-

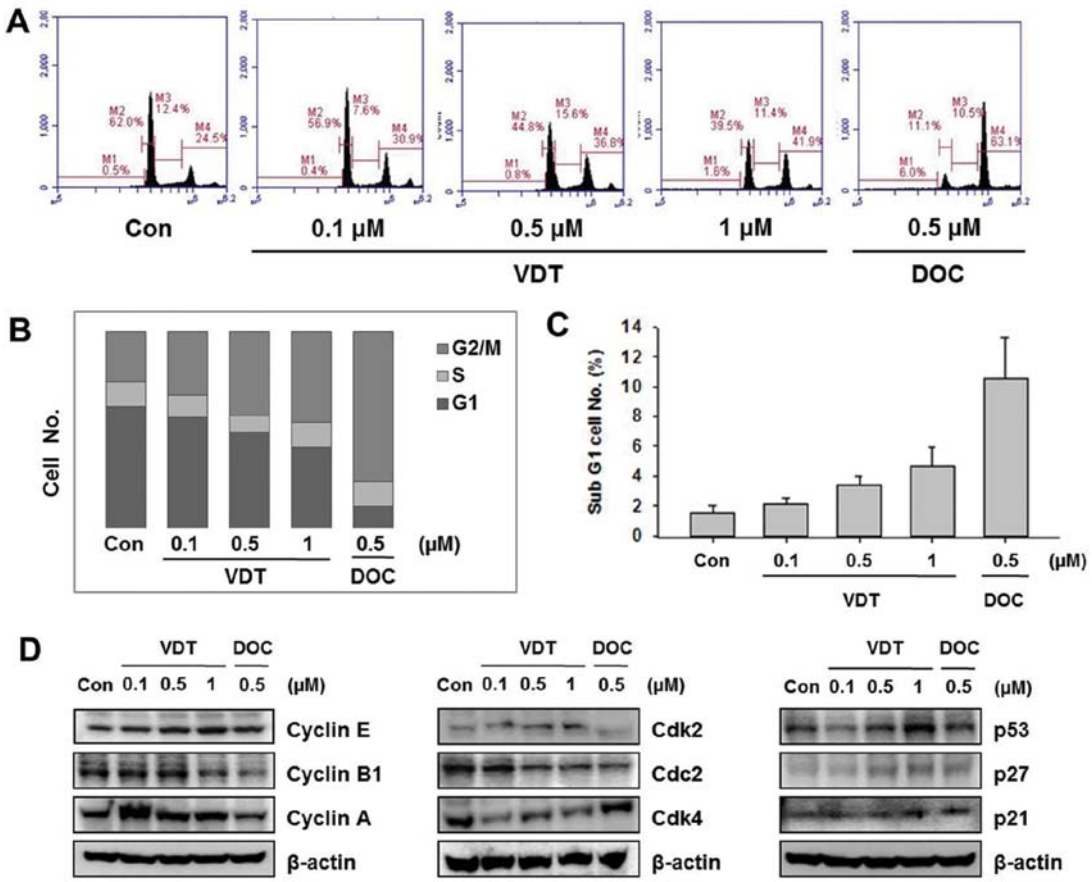

Figure 3. Effect of viriditoxin on cell cycle distribution and expression of cell cycle regulatory protein in LNCaP cells. Cells were treated for 48 h with the indicated concentrations of viriditoxin (VDT) or docetaxel (DOC), stained with propidium iodide (PI) and then analyzed by flow cytometry to determine the distribution of cells in each phase of the cell cycle. (A) Quantification of cell cycle distribution by flow cytometry. (B) Percentage of LNCaP cells following drug treatment. (C) Percentage of cells in the sub-G1 phase. (D) Effect of VDT and DOC on expression of cell cycle regulatory proteins. Cells were treated with the indicated concentrations of VDT for 48 h, harvested, and then western blot analysis was performed using the following antibodies: cyclin E, cyclin B1, cyclin A, Cdk2, Cdk4, Cdc2, p53, p21, p27 and actin as an internal loading control. All data are representative of three independent experiments.

sion, cells were treated with the indicated concentration of VDT (0.1, 0.5 and 1 μM) or DOC (0.5 μM) for 48 h and then flow cytometric analysis was performed. VDT significantly increased the percentage of cells in the G2/M phase and concomitantly decreased cells in the S phase in LNCaP cells (Fig. 3). LNCaP cells treated with 0.5 μM DOC completely arrested the G2/M phase resulting in 63.1% of cells in this phase (Fig. 3A). VDT also increased the proportion of cells in the sub-G1 phase, which is an apoptosis indicator in LNCaP cells (Fig. 3C). To explore the mechanism of VDT on regulation of the cell cycle, we examined the expression levels of cell cycle-related proteins by western blot analysis. Cell cycle progression is tightly regulated by cyclins and cyclin-dependent kinases (CDKs). Generally, the cyclin D1-CDK4 complex regulates the cell cycle at the G1 phase while the cyclin E-CDK2 complex initiates the G2/M transition. The CDK inhibitors p21Cip1 and p27Kip1 regulate cell cycle progression from the G0/G1 phase to the S phase; induction of p21Cip1 and p27Kip1 may lead to blockade of the G1/S transition (28-29). As shown in Fig. 3, VDT decreased expression levels of cyclin A, cyclin B1 and Cdc2, whereas expression of cyclin E1, Cdk2 was increased. In particular, VDT significantly increased expression of p27, p53 and p21 in a concentration-dependent manner in LNCaP cells (Fig. 3).

VDT slightly induces apoptosis in LNCaP cells. Annexin V-FITC-conjugated staining and western blot analysis were performed to evaluate induction of apoptosis in LNCaP cells after VDT treatment. Although a marked increase in concentration-dependent cell death was observed in the cytotoxicity assay, only a slight change in apoptotic cell death was detected at the highest concentration of VDT (Fig. 4A). DAPI staining was used to confirm the effect of VDT on apoptosis. Similar to observations of the sub-G1 phase of the cell cycle, VDT induce increase amount number of apoptotic nuclei (condensed or fragmented chromatin) compared to the untreated control which showed enhanced fluorescence with DAPI staining (Fig. 4B). Western blot analysis also showed that high concentrations of VDT increased cleaved PARP, Bax and cytochrome *c*, cleaved caspase-3 expression levels and decreased Bcl-2 expression significantly in LNCaP cells (Fig. 4C).

VDT induces autophagic cell death in LNCaP cells. To elucidate the cell death mechanism, we investigated autophagic cell death by western blot analysis and acridine orange staining. VDT significantly increased autophagic cell death in LNCaP cells. Conversion of the soluble form of LC3-I to the autophagic vesicle-associated form LC3-II is considered a specific marker

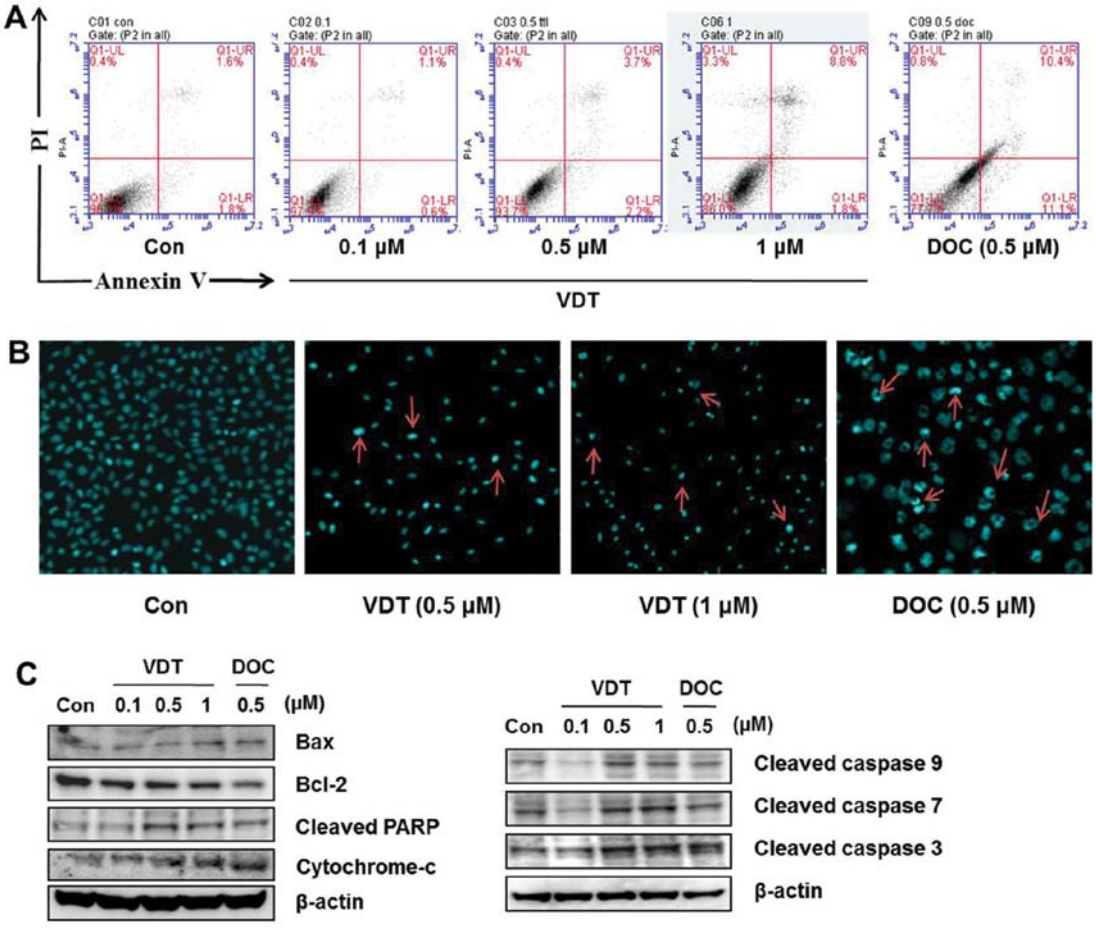

Figure 4. Effect of viriditoxin on apoptosis in LNCaP cells. (A) Annexin V-PI binding assay. Induction of apoptosis by viriditoxin (VDT) in LNCaP cells was examined by the Annexin V-PI binding assay. Cells were treated with VDT for 48 h at the different concentrations indicated. Late apoptosis was detected by flow cytometric analysis of Annexin V/PI-stained cells. (B) DAPI staining. VDT and docetaxel (DOC) induce nuclear morphological changes and apoptosis in LNCaP cells treated for 48 h with the indicated concentrations of drugs followed by fixation and DAPI staining. Apoptotic cells are marked by arrows. The images were captured at x10 magnification. (C) Western blot analysis. Effect of VDT and DOC on expression of proteins associated with apoptotic cell death. Protein levels were normalized by comparison with levels of β-actin.

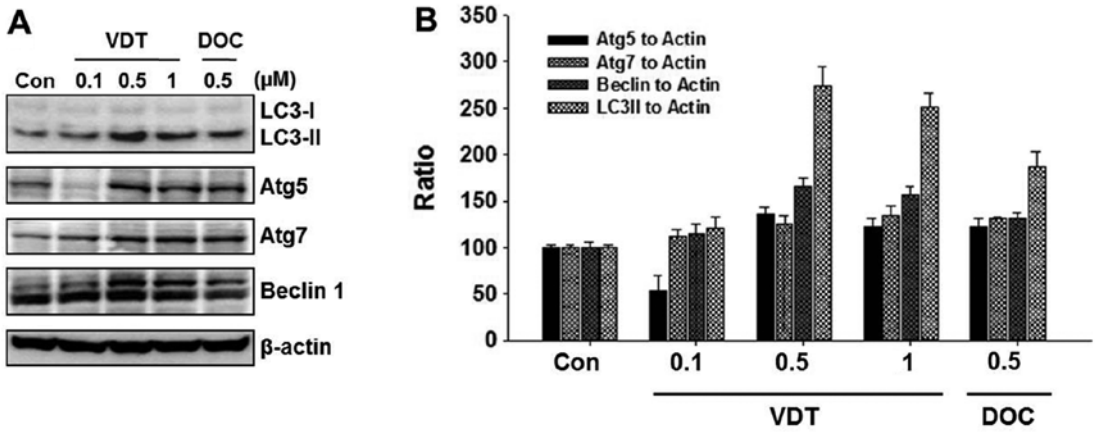

Figure 5. Effect of viriditoxin on expression of autophagy-related proteins in LNCaP cells. (A) Western blot analysis was performed with LC3, Beclin-1, ATG5 and ATG7 antibodies. Equal loading and transfer were verified by re-probing the membranes with β-actin antibody. (B) The ratio of conversion of LC3-II, Beclin-1, ATG5 and ATG7 to LC3-I and β-actin was calculated by densitometry.

of autophagosome production. As shown in Fig. 5A, VDT significantly increased the level of LC3-II, whereas unconjugated LC3-I levels were slightly decreased. In addition, beclin-1, Atg5 and Atg7 were required to initiate the formation of autophagosomes. Similar to LC3-II, the expression of beclin-1 was increased by VDT treatment (Fig. 5A). The ratio

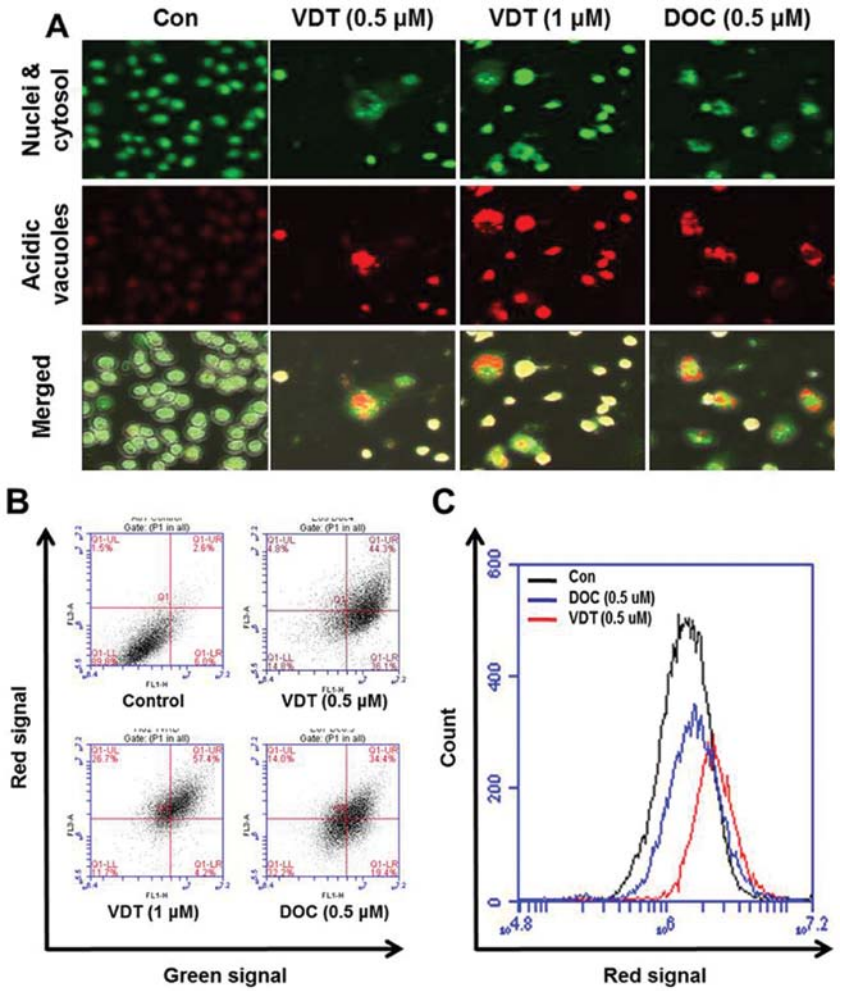

Figure 6. Visualization of intracellular autophagic vacuoles in LNCaP cells. (A) Immunofluorescence microscopy of acridine orange (AO)-stained LNCaP cells treated for 48 h with the indicated drugs (Olympus confocal microscope FV10i; x600, magnification). (B) Flow cytometric analysis after AO staining. (C) Histogram profiles of the control and the highest dose of drug were generated by flow cytometry.

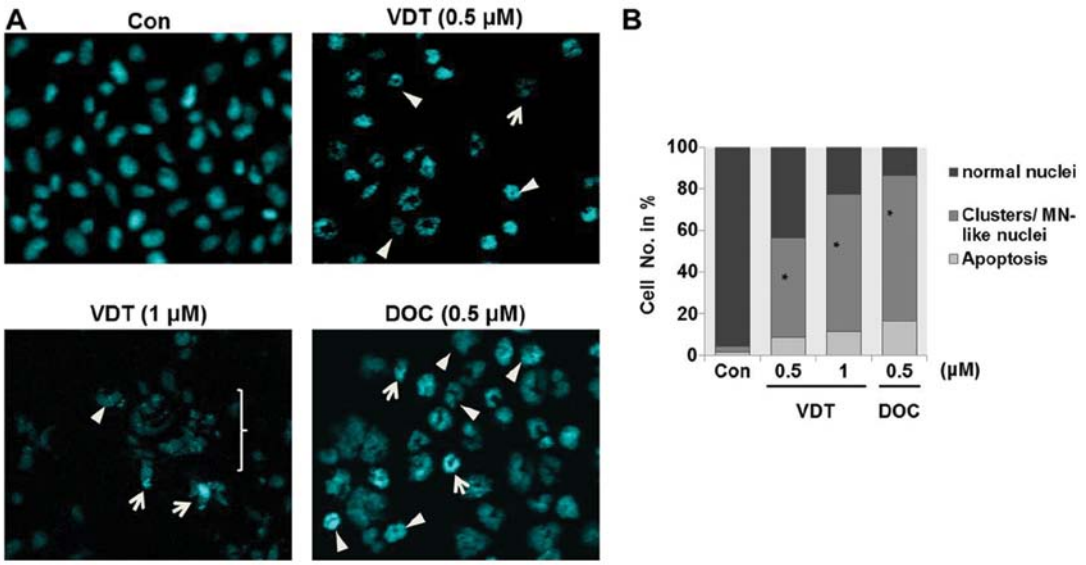

Figure 7. Effect of viriditoxin on mitotic catastrophe in LNCaP cells. (A) Changes in the nuclear morphology of cells exposed to the indicated concentrations of viriditoxin (VDT) or docetaxel (DOC) for 48 h was assessed by DAPI staining at x400, magnification. Mitotic catastrophe is characterized by multinucleated (MN) aberrant cells (arrowheads). Cells with condensed and fragmented chromatin are typical of apoptosis (arrows). The bracket indicates mitotic catastrophe-like clusters. In contrast, all control cell nuclei were separated and well-rounded. (B) Quantitation of the percentage of normal, MN and apoptotic cells according to different doses of drugs was determined by fluorescence microscopy analysis. Data is representative of five independent experiments. $^{*}p<0.05$.

of conversion of LC3-II, beclin-1, ATG5 and ATG7 to LC3-I and β-actin was calculated by densitometry (Fig. 5B).

Next, induction of autophagy was confirmed by acridine orange staining, which is commonly used to study autophagy. Acridine orange is a lysotropic dye that accumulates in acidic organelles in a pH-dependent manner. At neutral pH, acridine orange is a hydrophobic green fluorescent molecule. However, within acidic vesicles, acridine orange becomes protonated and trapped within the organelle and forms aggregates that emit bright red fluorescence (30). As shown in Fig. 6A, control cells primarily displayed green fluorescence with minimal red fluorescence, indicating a lack of acidic vesicular organelles (AVOs). However, drug-treated cells showed a fold-increase in red fluorescent AVOs at 48 h post-treatment compared to the controls (Fig. 6A). Flow cytometric analysis after acridine orange staining also showed an increase in red fluorescence intensity after drug treatment indicating enhancement of AVOs (Fig. 6B). Histogram profiles in Fig. 6C show the mean fluorescence intensity of control and drug-treated cells.

VDT induces mitotic catastrophe in LNCaP cells. Analysis of nuclear morphology by fluorescence microscopy showed that VDT significantly induced mitotic catastrophe in LNCaP cells. Mitotic catastrophe was clearly characterized by the appearance of enlarged multinucleated cells or aberrant nuclei clusters (Fig. 7A). Approximately 45 to 60% of cells showed different abnormalities of their nuclei compared to untreated control cells after treatment with VDT (Fig. 7B).

Discussion

Tubulin inhibitors used as drugs for cancer chemotherapy directly interfere with the tubulin system in multiple solid tumors. Recently, the development of tubulin inhibitors has been considerable interest because their function and biological properties interfere with microtubule formation by affecting polymerization or depolymerization of tubulin (31-33). The disruption of microtubule formation as a primary target for cancer chemotherapy can lead to cell cycle arrest in the M phase. The majority of compounds blocking microtubule formation are natural products that are remarkably diverse and have expanded chemical structures. A number of microtubule targeting chemotherapy drugs (paclitaxel, DOC or colchicine) are cytotoxic by stabilizing or destabilizing microtubules. These drugs bind to distinct sites on the microtubule or to the tubulin dimer and affect microtubule dynamics by blocking the G2/M phase, thus prolonging the pro/metaphase to anaphase transition time and inducing cell death (34-37).

VDT is a novel compound isolated from *Paecilomyces variotii* fungus (38) that inhibits FtsZ by affecting cell morphology, macromolecular synthesis, and responses to DNA damage; thus VDT has become a novel therapeutic target of antibiotics (8,39). However, there is no data on the antitumor activity of VDT. To clarify the molecular targets of VDT, we first examined its cytotoxicity and the effect on cell cycle progression in prostate cancer cells. VDT showed different sensitivity in the three types of prostate cancer cell lines evaluated in this study. LNCaP cells were very sensitive, DU145 cells were moderately sensitive, and PC3 cells showed low sensitivity. LNCaP cells were mostly inhibited in a concentration-dependent manner. Previous studies have indicated that chemotherapeutic agents activating p53 can induce both apoptosis and autophagic cell death in different cancer cells (40,41). We predicted that VDT could induce apoptotic cell death in LNCaP cells via p53-dependent induction of p21. To confirm that VDT induces apoptotic cell death, the Annexin V-FITC assay was performed. In this assay, a small amount of apoptosis was observed. VDT exerted a broad spectrum of effects on prostate cancer cells including arrest of the G2/M phase, p21 upregulation, and induction of apoptosis. A significant increase in cytochrome *c* release in the cytoplasm, cleavage of PARP, and caspase activation were observed in LNCaP cells after VDT treatment. In the present study, VDT induced significant increases in the population of cells in the G2/M phase. The G2/M transition of the mitotic cycle is controlled by the cyclin A/B-CDC2/1 complex and arrested by p21 (42,43). We found that VDT increased the expression of p21, p27 and Cdc 2 with similar changes in p53 expression and decreased cyclin B1/cyclin A levels, which indicated arrest of the G2/M phase in LNCaP cells. Several reports also demonstrated that the principal pro-apoptotic transcription factor, p53, can stimulate autophagy (44,45). Autophagy is mainly a catabolic mechanism by which cellular components are degraded through the action of lysosomes (46-49). However, there is currently a debate over the role of autophagy in ensuring continuous growth of cancer cells. Despite this lack of clarity, it is believed that autophagy plays an important role in cancer, both in protecting against cancer as well as potentially contributing to the growth of cancer (50).

Although most of the microtubule targeting drugs inhibits cancer cells through the apoptosis pathway, some can inhibit apoptotic cell death in wild-type p53 prostate and colorectal cancer cells (15). Microtubule disrupting drugs can also trigger cell death via the mitotic catastrophe pathway (51). The DNA damage response and cell cycle checkpoints of cancer cells make them more susceptible to mitotic catastrophe (52). Our data indicated that VDT markedly increased cytotoxicity through apoptosis and mitotic catastrophe in LNCaP cells. Previous studies also showed that various tubulin-binding drugs, such as vinblastine, naphthazarin or 2-methoxyestradiol, contribute to anticancer activity by stimulating autophagic cell death in different cancer cell lines (24,25,53-55). Specifically, vinblastine has been shown to increase formation of autophagosomes as is indicated by increased levels of autophagic cell death (56,57). In the present study, we evaluated VDT as a microtubule targeting agent and clearly showed that it induced autophagic cell death. To confirm the mechanism underlying the autophagic cell death pathway, we investigated whether any functional links between microtubules and autophagic cell death exist. Similarly, other studies have also tried to gain insights/knowledge on the mechanisms underlying the association between microtubule targeting drugs and autophagy. LC31A/1B is a microtubule-associated protein (MAP) (58). Moreover, both LC31 and lapidated LC3II are found in subcellular fractions containing fragments of microtubules, suggesting an interaction between LC3 and microtubules (59). Therefore, we predict that tubulin- or microtubulin-targeting drugs may impact the initiation and termination of autophagy by releasing LC3 into the cytoplasm. A previous study showed a similar association between LC3 and autophagy, concluding

that LC3 must be released from microtubules to participate in the initiation of autophagy (60). However, several previous studies using different microtubule-associated agents including taxol or nocodazole denied the participation of microtubules in autophagosome formation in different cancer cell lines (22,24,61). In contrast, disassembling microtubules treated with high doses of nocodazole was shown to prevent autophagosome formation, thus highlighting the function of microtubules in autophagy (23). In addition, another study showed that vinca alkaloid enhances autophagosome formation (24). Recently, microtubules have been suggested as global and local integrators of autophagic responses in the formation and motility of autophagosomes rather than in their fusion with lysosomes (62).

In conclusion, our data showed that VDT significantly inhibited proliferation of prostate cancer cells and induced autophagic cell death in LNCaP cells via disturbance of tubulin formation. Further studies are necessary to better understand the effect of autophagy inhibition on autophagosome production and lysosomal degradation. However, the results of the present study highlight autophagic cell death following VDT treatment in LNCaP cells and also predict a functional relationship between microtubules and autophagy in the context of anticancer chemotherapy. Furthermore, we also showed that VDT treatment induced slight apoptosis and cell death via the mitotic catastrophe pathway. Despite the promise of VDT treatment demonstrated here, further investigation is necessary to elucidate the relationship between autophagy and microtubules after VDT treatment in LNCaP cells.

Acknowledgements

This study was supported in part by the Korea Research Foundation (KRF-2013-041-E00392) grant funded by the Korean Government.

References

1. Jemal A, Bray F, Center MM, Ferly J, Ward E and Forman D: Global cancer statistics. CA Cancer J Clin 6: 69-90, 2011.
2. Siegel R, Ward E, Brawley O and Jemal A: Cancer statistics, 2011: the impact of eliminating socioeconomic and racial disparities on premature cancer deaths. CA Cancer J Clin 6: 212-236, 2011.
3. Riihimäki M, Thomsen H, Brandt A, Sundquist J and Hemminki K: What do prostate cancer patients die of? Oncologist 16: 175-181, 2011.
4. Hsing AW and Chokkalingam AP: Prostate cancer epidemiology. Front Biosci 11: 1388-1413, 2006.
5. Parent ME and Siemiatycki J: Occupation and prostate cancer. Epidemiol Rev 23: 138-143, 2001.
6. Lock RL and Harry EJ: Cell-division inhibitors: new insights for future antibiotics. Nat Rev Drug Discov 7: 324-338, 2008.
7. Erickson HP, Anderson DE and Osawa M: FtsZ in bacterial cytokinesis: cytoskeleton and force generator all in one. Microbiol Mol Biol Rev 74: 504-528, 2010.
8. Wang J, Galgoci A, Kodali S, Herath KB, Jayasuriya H, Dorso K, Vicente F, Gonzalez A, Cully D, Bramhill D and Singh S: Discovery of a small molecule that inhibits cell division by blocking FtsZ, a novel therapeutic target of antibiotics. J Biol Chem 278: 44424-44428, 2003.
9. Löwe J and Amos LA: Crystal structure of the bacterial cell-division protein FtsZ. Nature 391: 203-206, 1998.
10. Chung KS, Yim NH, Lee SH, Choi SJ, Hur KS, Hoe KL, Kim DU, Goehle S, Kim HB, Song KB, Yoo HS, Bae KH, Simon J and Won M: Identification of small molecules inducing apoptosis by cell-based assay using fission yeast deletion mutants. Invest New Drugs 26: 299-307, 2008.
11. Heggeness MH, Simon M and Singer SJ: Association of mitochondria with microtubules in cultured cells. Proc Natl Acad Sci 75: 3863-3866, 1978.
12. Diaz JF and Andreu JM: Assembly of purified GDP-tubulin into microtubules induced by taxol and taxotere: reversibility, ligand stoichiometry, and competition. Biochemistry 32: 2747-2755, 1993.
13. Lavelle F, Bissery MC, Combeau C, Riou JF, Vrignaud P and André S: Preclinical evaluation of docetaxel (Taxotere). Semin Oncol 22: 3-16, 1995.
14. Stein CA: Mechanisms of action of taxanes in prostate cancer. Semin Oncol 26: 3-7, 1999.
15. Kim JY, Chung JY, Lee SG, Kim YJ, Park JE, Yun J, Park YC, Kim BG, Yoo YH and Kim JM: p53 interferes with microtubule-stabilizing agent-induced apoptosis in prostate and colorectal cancer cells. Int J Mol Med 31: 1388-1394, 2013.
16. Wolter KG, Hsu YT, Smith CL, Nechushtan A, Xi XG and Youle RJ: Movement of Bax from the cytosol to mitochondria during apoptosis. J Cell Biol 139: 1281-1292, 1997.
17. Saunders DE, Lawrence WD, Christensen C, Wappler NL, Ruan H and Deppe G: Paclitaxel-induced apoptosis in MCF-7 breast-cancer cells. Int J Cancer 70: 214-220, 1997.
18. Lin HL, Liu TY, Chau GY, Lui WY and Chi CW: Comparison of 2-methoxyestradiol-induced, docetaxel-induced, and paclitaxel-induced apoptosis in hepatoma cells and its correlation with reactive oxygen species. Cancer 89: 983-994, 2000.
19. Vakifahmetoglu H, Olsson M and Zhivotovsky B: Death through a tragedy: mitotic catastrophe. Cell Death Differ 15: 1153-1162, 2008.
20. Roninson IB, Broude EV and Chang BD: If not apoptosis, then what? Treatment-induced senescence and mitotic catastrophe in tumor cells. Drug Resist Updat 4: 303-313, 2001.
21. Alotaibi MR, Asnake B, Di X, Beckman MJ, Durrant D, Simoni D, Baruchello R, Lee RM, Schwartz EL and Gewirtz DA: Stilbene 5c, a microtubule poison with vascular disrupting properties that induces multiple modes of growth arrest and cell death. Biochem Pharmacol 86: 1688-1698, 2013.
22. Aplin A, Jasionowski T, Tuttle DL, Lenk SE and Dunn WA Jr: Cytoskeletal elements are required for the formation and maturation of autophagic vacuoles. J Cell Physiol 152: 458-466, 1992.
23. Fass E, Shvets E, Degani I, Hirschberg K and Elazar Z: Microtubules support production of starvation-induced autophagosomes but not their targeting and fusion with lysosomes. J Biol Chem 281: 36303-36316, 2006.
24. Kochl R, Hu XW, Chan EY and Tooze SA: Microtubules facilitate autophagosome formation and fusion of autophagosomes with endosomes. Traffic 7: 129-145, 2006.
25. Acharya BR, Bhattacharyya S, Choudhury D and Chakrabarti G: The microtubule depolymerizing agent naphthazarin induces both apoptosis and autophagy in A549 lung cancer cells. Apoptosis 16: 924-939, 2011.
26. Xie R, Nguyen S, McKeehan WL and Liu L: Acetylated microtubules are required for fusion of autophagosomes with lysosomes. BMC Cell Biol 11: 89-100, 2010.
27. Mansila S, Bataller M and Portugal J: Mitotic catastrophe as a consequence of chemotherapy. Anticancer Agents Med Chem 6: 589-602, 2006.
28. Harper JW, Adami GR, Wei N, Keyomarsi K and Elledge SJ: The p21 Cdk-interacting protein Cip1 is a potent inhibitor of G1 cyclin-dependent kinases. Cell 75: 805-816, 1993.
29. Grimmler M, Wang Y, Mund T, Ciliensek Z, Keidel EM, Waddell MB, Jäkel H, Kullmann M, Kriwacki RW and Hengst L: Cdk-inhibitory activity and stability of p27Kip1 are directly regulated by oncogenic tyrosine kinases. Cell 128: 269-280, 2007.
30. Millot C, Millot JM, Morjani H, Desplaces A and Manfait M: Characterization of acidic vesicles in multidrug-resistant and sensitive cancer cells by acridine orange staining and confocal micro spectrofluorometry. J Histochem Cytochem 45: 1255-1264, 1997.
31. Perez EA: Microtubule inhibitors: differentiating tubulin-inhibiting agents based on mechanisms of action, clinical activity, and resistance. Mol Cancer Ther 8: 2086-2095, 2009.
32. Lu Y, Chen J, Xiao M, Li W and Miller DD: An overview of tubulin inhibitors that interact with the colchicine binding site. Pharm Res 29: 2943-2971, 2012.
33. Longuet M, Serduc R and Riva C: Implication of bax in apoptosis depends on microtubule network mobility. Int J Oncol 25: 309-317, 2004.

34. Botta M, Forli S, Magnani M and Manetti F: Molecular modeling approaches to study the binding mode on tubulin of microtubule destabilizing and stabilizing agents. Top Curr Chem 286: 279-328, 2009.
35. Georgiadis MS, Russell EK, Gazdar AF and Johnson BE: Paclitaxel cytotoxicity against human lung cancer cell lines increases with prolonged exposure durations. Clin Cancer Res 3: 449-454, 1997.
36. Checchi PM, Nettles JH, Zhou J, Snyder JP and Joshi HC: Microtubule-interacting drugs for cancer treatment. Trends Pharmacol Sci 24: 361-365, 2003.
37. Hernandez-Vargas H, Palacios J and Moreno-Bueno G: Molecular profiling of docetaxel cytotoxicity in breast cancer cells: uncoupling of aberrant mitosis and apoptosis. Oncogene 26: 2902-2913, 2007.
38. Silva MRO, Kawai K, Hosoe T, Takaki GMC, Gusmão NB and Fukushima K: Viriditoxin, an antibacterial substance produced by mangrove endophytic fungus *Paecilomyces variotii*. In: Microbial Pathogens and Strategies for Combating Them: Science, Technology and Education. Méndez-Vilas A (ed), Formatex Research Center, Badajoz, pp1406-1411, 2013.
39. Park YS, Grove CI, González-López M, Urgaonkar S, Fettinger JC and Shaw JT: Synthesis of (-)-viriditoxin: a 6,6'-binaphthopyran-2-one that targets the bacterial cell division protein FtsZ. Angew Chem Int Ed Engl 50: 3730-3733, 2011.
40. Feng Z, Zhang H, Levine AJ and Jin S: The coordinate regulation of the p53 and mTOR pathways in cells. Proc Natl Acad Sci 102: 8204-8209, 2005.
41. Brady CA and Attardi LD: p53 at a glance. J Cell Sci 123: 2527-2532, 2010.
42. Eastman A: Cell cycle checkpoints and their impact on anticancer therapeutic strategies. J Cell Biochem 91: 223-231, 2004.
43. Payne SR, Zhang S, Tsuchiya K, Moser R, Gurley KE, Longton G, deBoer J and Kemp CJ: p27kip1 deficiency impairs G2/M arrest in response to DNA damage, leading to an increase in genetic instability. Mol Cell Biol 28: 258-268, 2008.
44. Maiuri MC, Galluzzi L, Morselli E, Kepp O, Malik SA and Kroemer G: Autophagy regulation by p53. Curr Opin Cell Biol 22: 181-185, 2010.
45. Tasdemir E, Maiuri MC, Galluzzi L, Vitale I, Djavaheri-Mergny M, D'Amelio M, Criollo A, Morselli E, Zhu C, Harper F, Nannmark U, Samara C, Pinton P, Vicencio JM, Carnuccio R, Moll UM, Madeo F, Paterlini-Brechot P, Rizzuto R, Szabadkai G, Pierron G, Blomgren K, Tavernarakis N, Codogno P, Cecconi F and Kroemer G: Regulation of autophagy by cytoplasmic p53. Nat Cell Biol 10: 676-687, 2008.
46. Lin NY, Beyer C, Giessl A, Kireva T, Scholtysek C, Uderhardt S, Munoz LE, Dees C, Distler A, Wirtz S, Krönke G, Spencer B, Distler O, Schett G and Distler JH: Autophagy regulates TNFα-mediated joint destruction in experimental arthritis. Ann Rheum Dis 72: 761-768, 2013.
47. Klionsky DJ: The molecular machinery of autophagy: unanswered questions. J Cell Sci 118: 7-18, 2005.
48. Klionsky DJ: Autophagy: from phenomenology to molecular understanding in less than a decade. Nat Rev Mol Cell Biol 8: 931-937, 2007.
49. Mizushima N and Klionsky DJ: Protein turnover via autophagy: implications for metabolism. Annu Rev Nutr 27: 19-40, 2007.
50. Shimizu S, Yoshida T, Tsujioka M and Arakawa S: Autophagic cell death and cancer. Int J Mol Sci 15: 3145-3153, 2014.
51. Nabha SM, Mohammad RM, Dandashi MH, Coupaye-Gerard B, Aboukameel A, Pettit GR and Al-Katib AM: Combretastatin-A4 prodrug induces mitotic catastrophe in chronic lymphocytic leukemia cell line independent of caspase activation and poly (adp-ribose) polymerase cleavage. Clin Cancer Res 8: 2735-2741, 2002.
52. Burns TF, Fei P, Scata KA, Dicker DT and El-Deiry WS: Silencing of the novel p53 target gene Snk/Plk2 leads to mitotic catastrophe in paclitaxel (taxol)-exposed cells. Mol Cell Biol 23: 5556-5571, 2003.
53. Chen Y, McMillan-Ward E, Kong J, Israels SJ and Gibson SB: Oxidative stress induces autophagic cell death independent of apoptosis in transformed and cancer cells. Cell Death Differ 15: 171-182, 2008.
54. Kamath K, Okouneva T, Larson G, Panda D, Wilson L and Jordan MA: 2-Methoxyestradiol suppresses microtubule dynamics and arrests mitosis without depolymerizing microtubules. Mol Cancer Ther 5: 2225-2233, 2006.
55. Lorin S, Borges A, Ribeiro Dos Santos L, Souquere S, Pierron G, Ryan KM, Codogno P and Djavaheri-Mergny M: c-Jun NH2-terminal kinase activation is essential for DRAM-dependent induction of autophagy and apoptosis in 2-methoxyestradiol-treated Ewing sarcoma cells. Cancer Res 69: 6924-6931, 2009.
56. Arstila AU, Nuuja IJ and Trump BF: Studies on cellular autophagocytosis: vinblastine-induced autophagy in the rat liver. Exp Cell Res 87: 249-252, 1974.
57. Marzella L, Sandberg PO and Glaumann H: Autophagic degradation in rat liver after vinblastine treatment. Exp Cell Res 128: 291-301, 1980.
58. Tanida I, Ueno T and Kominami E: LC3 and autophagy. Methods Mol Biol 445: 77-88, 2008.
59. Geeraert C, Ratier A, Pfisterer SG, Perdiz D, Cantaloube I, Rouault A, Pattingre S, Proikas-Cezanne T, Codogno P and Pous C: Starvation-induced hyperacetylation of tubulin is required for the stimulation of autophagy by nutrient deprivation. J Biol Chem 285: 24184-24194, 2010.
60. Shen S, Kepp O, Martins I, Vitale I, Souquère S, Castedo M, Pierron G and Kroemer G: Defective autophagy associated with LC3 puncta in epothilone-resistant cancer cells. Cell Cycle 9: 377-383, 2010.
61. Reunanen H, Marttinen M and Hirsimaki P: Effects of griseofulvin and nocodazole on the accumulation of autophagic vacuoles in Ehrlich ascites tumor cells. Exp Mol Pathol 48: 97-102, 1988.
62. Mackeh R, Perdiz D, Lorin S, Codogno P and Pous C: Autophagy and microtubules - new story, old players. J Cell Sci 126: 1071-1080, 2013.